Journal of Zhejiang University SCIENCE A
ISSN 1673-565X (Print); ISSN 1862-1775 (Online)
www.zju.edu.cn/jzus; www.springerlink.com
E-mail: jzus@zju.edu.cn

Adaptive rotor current control for wind-turbine driven DFIG using resonant controllers in a rotor rotating reference frame*

Jia-bing HU, Yi-kang HE, Hong-sheng WANG
(*School of Electrical Engineering, Zhejiang University, Hangzhou 310027, China*)
E-mail: emec_zju@zju.edu.cn; ykhe@zju.edu.cn; homeson_ee@hotmail.com
Received Oct. 8, 2007; revision accepted Nov. 26, 2007; published online Jan. 11, 2008

Abstract: This paper proposes an adaptive rotor current controller for doubly-fed induction generator (DFIG), which consists of a proportional (P) controller and two harmonic resonant (R) controllers implemented in the rotor rotating reference frame. The two resonant controllers are tuned at slip frequencies ω_{slip+} and ω_{slip-}, respectively. As a result, the positive- and negative-sequence components of the rotor current are fully regulated by the PR controller without involving the positive- and negative-sequence decomposition, which in effect improves the fault ride-through (FRT) capability of the DFIG-based wind power generation system during the period of large transient grid voltage unbalance. Correctness of the theoretical analysis and feasibility of the proposed unbalanced control scheme are validated by simulation on a 1.5-MW DFIG wind power generation system.

Key words: Unbalanced grid voltage, Doubly-fed induction generator (DFIG), Proportional plus Resonant (PR) controller, Fault ride-through (FRT)
doi:10.1631/jzus.A073026 **Document code:** A **CLC number:** TM315; TM614

INTRODUCTION

Wind turbines based on doubly-fed induction generators (DFIGs) with converters rated at around 25%~30% of the generator rating are becoming increasingly popular. Compared with the wind turbines using fixed speed induction generators or fully-fed synchronous generators with full-sized converters, the DFIG-based wind turbines offer not only the advantages of variable speed operation and four-quadrant active and reactive power capabilities, but also lower converter cost and power losses. However, both transmission and distribution networks could usually have small steady state and large transient voltage unbalance. If voltage unbalance is not considered by the DFIG control system, the stator current could become highly unbalanced even with a small unbalanced stator voltage. The unbalanced currents create unequal heating on the stator windings, and pulsations in the electromagnetic torque and stator output active and reactive powers (Hu *et al*., 2007; Xu and Wang, 2007).

System control and operation of the wind-turbine driven DFIG under unbalanced grid voltage conditions were studied (Chomat *et al*., 2002; Brekken and Mohan, 2003; Brekken *et al*., 2005; Jang *et al*., 2006; Hu *et al*., 2007; Xu and Wang, 2007; Wang and Xu, 2007). In (Brekken and Mohan, 2003; Brekken *et al*., 2005), the control of DFIG for the compensation of torque pulsations was investigated. The required rotor compensating voltage was generated either directly according to the torque pulsations (Brekken *et al*., 2005) or from the calculated compensating currents (Brekken and Mohan, 2003), both of which fluctuated at twice the grid frequency. As a result, the current controller must be carefully tuned to provide the required system response. In (Chomat *et al*., 2002; Jang *et al*., 2006), an extended vector control of doubly fed machine under unbalanced network conditions was proposed, which was implemented in the positive and negative synchronous reference frames, and provided an improved control for the stator currents and the active and reactive powers. In (Hu *et al*., 2007; Xu

* Project (No. 50577056) supported by the National Natural Science Foundation of China

and Wang, 2007; Wang and Xu, 2007), the authors investigated the impact of unbalanced stator voltage on the pulsations of stator and rotor currents, electromagnetic torque and stator active and reactive powers in detail. Similar to (Chomat *et al*., 2002; Jang *et al*., 2006), a dual rotor current controller based on the decomposing of positive- and negative-sequence components was employed, via stator flux orientation (SFO) (Xu and Wang, 2007) and stator voltage orientation (SVO) (Hu *et al*., 2007; Wang and Xu, 2007), respectively, to control the rotor positive- and negative-sequence currents. Since the decomposing process involves considerable time delay, which brings errors in the amplitude and phase of the decomposed variables, the systems cannot be fully decoupled during transient conditions. Consequently, the system performance and stability are all degraded naturally. Furthermore, even when the grid voltage is perfectly balanced, the control system still has to perform the decomposing of the positive- and negative-sequence rotor currents with low-pass or notch filter, which unnecessarily deteriorates the transient performance of the whole control system.

Based on the DFIG model presented by Hu *et al*.(2007), this paper proposes an adaptive rotor current controller for wind-turbine driven DFIG, which consists of a proportional (P) controller and two harmonic resonant (R) controllers implemented in the rotor rotating reference frame. The two resonant controllers are tuned at the slip frequencies of $\omega_{\text{slip+}}$ and $\omega_{\text{slip–}}$, respectively. As a result, the positive- and negative-sequence components of the rotor current are fully regulated without involving the positive- and negative-sequence decomposition. Correctness of the theoretical analysis and feasibility of the proposed unbalanced control scheme are validated by simulation on a 1.5-MW DFIG wind power generation system during the period of large transient grid voltage unbalance.

DFIG MODEL IN ROTOR ROTATING FRAME

A detailed study of the DFIG system behavior under unbalanced stator voltage condition has been presented in (Hu *et al*., 2007). Thus, a description for deducing electromagnetic torque and instantaneous stator output active and reactive powers under unbalanced grid voltage conditions is not included here.

Fig.1 shows the generalized equivalent circuit of a DFIG represented in the rotor reference frame rotating at the angular speed of ω_{r}. During stator voltage unbalance, the stator and rotor voltage, current and flux contain both positive- and negative-sequence components. According to Fig.1, the stator and rotor voltage and flux are given, respectively, by

$$\boldsymbol{V}^{\text{r}}_{\text{s}\alpha\beta}=R_{\text{s}}\boldsymbol{I}^{\text{r}}_{\text{s}\alpha\beta}+\frac{\text{d}\boldsymbol{\psi}^{\text{r}}_{\text{s}\alpha\beta}}{\text{d}t}+\text{j}\omega_{\text{r}}\boldsymbol{\psi}^{\text{r}}_{\text{s}\alpha\beta}, \tag{1a}$$

$$\boldsymbol{V}^{\text{r}}_{\text{r}\alpha\beta}=R_{\text{r}}\boldsymbol{I}^{\text{r}}_{\text{r}\alpha\beta}+\frac{\text{d}\boldsymbol{\psi}^{\text{r}}_{\text{r}\alpha\beta}}{\text{d}t}, \tag{1b}$$

$$\boldsymbol{\psi}^{\text{r}}_{\text{s}\alpha\beta}=L_{\text{s}}\boldsymbol{I}^{\text{r}}_{\text{s}\alpha\beta}+L_{\text{m}}\boldsymbol{I}^{\text{r}}_{\text{r}\alpha\beta}, \tag{2a}$$

$$\boldsymbol{\psi}^{\text{r}}_{\text{r}\alpha\beta}=L_{\text{r}}\boldsymbol{I}^{\text{r}}_{\text{r}\alpha\beta}+L_{\text{m}}\boldsymbol{I}^{\text{r}}_{\text{s}\alpha\beta}, \tag{2b}$$

where, R_{s} and R_{r} are stator resistance and rotor resistance, respectively; $L_{\text{s}}=L_{\sigma\text{s}}+L_{\text{m}}$ and $L_{\text{r}}=L_{\sigma\text{r}}+L_{\text{m}}$ are the total self-inductance of stator and rotor windings, respectively; $L_{\sigma\text{s}}$, $L_{\sigma\text{r}}$ and L_{m} are stator and rotor leakage inductances and mutual inductance, respectively; ω_{r} is rotor angular speed; superscript r represents the rotor rotating reference frame.

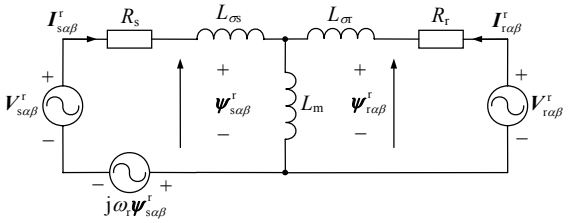

Fig.1 DFIG equivalent circuit in the rotor reference frame rotating at ω_{r}

According to Eqs.(2a) and (2b), the rotor flux can be expressed using stator flux and rotor current as

$$\boldsymbol{\psi}^{\text{r}}_{\text{r}\alpha\beta}=\sigma L_{\text{r}}\boldsymbol{I}^{\text{r}}_{\text{r}\alpha\beta}+L_{\text{m}}\boldsymbol{\psi}^{\text{r}}_{\text{s}\alpha\beta}/L_{\text{s}}, \tag{3}$$

where $\sigma=1-L_{\text{m}}^2/(L_{\text{s}}L_{\text{r}})$ is the leakage factor.

From Eq.(1a), there is

$$\frac{\text{d}\boldsymbol{\psi}^{\text{r}}_{\text{s}\alpha\beta}}{\text{d}t}=\boldsymbol{V}^{\text{r}}_{\text{s}\alpha\beta}-R_{\text{s}}\boldsymbol{I}^{\text{r}}_{\text{s}\alpha\beta}-\text{j}\omega_{\text{r}}\boldsymbol{\psi}^{\text{r}}_{\text{s}\alpha\beta}. \tag{4}$$

Substituting Eq.(3) and Eq.(4) into Eq.(1b) yields

$$\begin{aligned}\boldsymbol{V}^{\text{r}}_{\text{r}\alpha\beta}=&R_{\text{r}}\boldsymbol{I}^{\text{r}}_{\text{r}\alpha\beta}+\sigma L_{\text{r}}\frac{\text{d}\boldsymbol{I}^{\text{r}}_{\text{r}\alpha\beta}}{\text{d}t}+\\&(\boldsymbol{V}^{\text{r}}_{\text{s}\alpha\beta}-R_{\text{s}}\boldsymbol{I}^{\text{r}}_{\text{s}\alpha\beta}-\text{j}\omega_{\text{r}}\boldsymbol{\psi}^{\text{r}}_{\text{s}\alpha\beta})L_{\text{m}}/L_{\text{s}}.\end{aligned} \tag{5}$$

Under unbalanced conditions, a convenient way to model a DFIG is to use positive reference frame, rotating at the speed of ω_s, and a negative reference frame, rotating at the speed of $-\omega_s$ (Hu *et al*., 2007). The spatial relationships of various reference frames are shown in Fig.2.

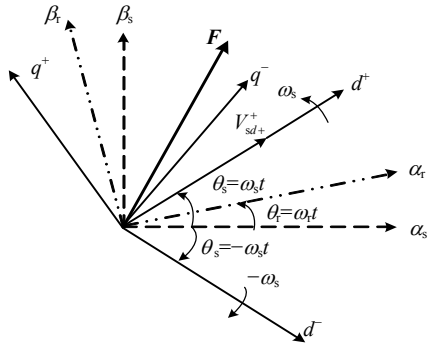

Fig.2 Relationships between the $\alpha_s\beta_s$, $\alpha_r\beta_r$, and the d^+q^+ and d^-q^- reference frames

According to Fig.2, the transformation between the $\alpha_s\beta_s$, $\alpha_r\beta_r$, and the d^+q^+ and d^-q^- reference frames are given by

$$\boldsymbol{F}_{dq}^{+}=\boldsymbol{F}_{\alpha\beta}^{\mathrm{s}}\mathrm{e}^{-\mathrm{j}\omega_s t},\quad \boldsymbol{F}_{dq}^{-}=\boldsymbol{F}_{\alpha\beta}^{\mathrm{s}}\mathrm{e}^{\mathrm{j}\omega_s t}, \tag{6a}$$

$$\boldsymbol{F}_{dq}^{+}=\boldsymbol{F}_{dq}^{-}\mathrm{e}^{-\mathrm{j}2\omega_s t},\quad \boldsymbol{F}_{dq}^{-}=\boldsymbol{F}_{dq}^{+}\mathrm{e}^{\mathrm{j}2\omega_s t}, \tag{6b}$$

$$\boldsymbol{F}_{dq}^{+}=\boldsymbol{F}_{\alpha\beta}^{\mathrm{r}}\mathrm{e}^{-\mathrm{j}\omega_{\mathrm{slip}+} t},\quad \boldsymbol{F}_{dq}^{-}=\boldsymbol{F}_{\alpha\beta}^{\mathrm{r}}\mathrm{e}^{\mathrm{j}\omega_{\mathrm{slip}-} t}, \tag{6c}$$

where superscripts +, − represent the positive- and negative-rotating reference frames, respectively; $\omega_{\mathrm{slip}+}=\omega_s-\omega_r$, $\omega_{\mathrm{slip}-}=-\omega_s-\omega_r$.

Thus according to Eq.(6) and Fig.2, the stator and rotor current, voltage and flux can be expressed in terms of positive- and negative-sequence components in the positive and negative reference frames, respectively, as

$$\begin{cases}
\boldsymbol{V}_{s\alpha\beta}^{\mathrm{r}}=\boldsymbol{V}_{s\alpha\beta+}^{\mathrm{r}}+\boldsymbol{V}_{s\alpha\beta-}^{\mathrm{r}}=\boldsymbol{V}_{sdq+}^{+}\mathrm{e}^{\mathrm{j}\omega_{\mathrm{slip}+}t}+\boldsymbol{V}_{sdq-}^{-}\mathrm{e}^{\mathrm{j}\omega_{\mathrm{slip}-}t},\\
\boldsymbol{I}_{s\alpha\beta}^{\mathrm{r}}=\boldsymbol{I}_{s\alpha\beta+}^{\mathrm{r}}+\boldsymbol{I}_{s\alpha\beta-}^{\mathrm{r}}=\boldsymbol{I}_{sdq+}^{+}\mathrm{e}^{\mathrm{j}\omega_{\mathrm{slip}+}t}+\boldsymbol{I}_{sdq-}^{-}\mathrm{e}^{\mathrm{j}\omega_{\mathrm{slip}-}t},\\
\boldsymbol{\psi}_{s\alpha\beta}^{\mathrm{r}}=\boldsymbol{\psi}_{s\alpha\beta+}^{\mathrm{r}}+\boldsymbol{\psi}_{s\alpha\beta-}^{\mathrm{r}}=\boldsymbol{\psi}_{sdq+}^{+}\mathrm{e}^{\mathrm{j}\omega_{\mathrm{slip}+}t}+\boldsymbol{\psi}_{sdq-}^{-}\mathrm{e}^{\mathrm{j}\omega_{\mathrm{slip}-}t},\\
\boldsymbol{V}_{r\alpha\beta}^{\mathrm{r}}=\boldsymbol{V}_{r\alpha\beta+}^{\mathrm{r}}+\boldsymbol{V}_{r\alpha\beta-}^{\mathrm{r}}=\boldsymbol{V}_{rdq+}^{+}\mathrm{e}^{\mathrm{j}\omega_{\mathrm{slip}+}t}+\boldsymbol{V}_{rdq-}^{-}\mathrm{e}^{\mathrm{j}\omega_{\mathrm{slip}-}t},\\
\boldsymbol{I}_{r\alpha\beta}^{\mathrm{r}}=\boldsymbol{I}_{r\alpha\beta+}^{\mathrm{r}}+\boldsymbol{I}_{r\alpha\beta-}^{\mathrm{r}}=\boldsymbol{I}_{rdq+}^{+}\mathrm{e}^{\mathrm{j}\omega_{\mathrm{slip}+}t}+\boldsymbol{I}_{rdq-}^{-}\mathrm{e}^{\mathrm{j}\omega_{\mathrm{slip}-}t},\\
\boldsymbol{\psi}_{r\alpha\beta}^{\mathrm{r}}=\boldsymbol{\psi}_{r\alpha\beta+}^{\mathrm{r}}+\boldsymbol{\psi}_{r\alpha\beta-}^{\mathrm{r}}=\boldsymbol{\psi}_{rdq+}^{+}\mathrm{e}^{\mathrm{j}\omega_{\mathrm{slip}+}t}+\boldsymbol{\psi}_{rdq-}^{-}\mathrm{e}^{\mathrm{j}\omega_{\mathrm{slip}-}t},
\end{cases} \tag{7}$$

where subscripts +, − represent the positive- and negative-sequence components, respectively.

SYSTEM CONTROL DESIGN

In this section, firstly, with maintaining the constant electromagnetic torque (Xu and Wang, 2007) selected as the control target for DFIG under unbalanced grid voltage condition, a novel rotor current controller implemented in the rotor rotating reference frame is proposed and designed without involving the decomposition of positive- and negative-sequence rotor currents. Then, an enhanced unbalanced control scheme for a DFIG-based wind power generation system is provided.

As shown in Fig.2, since the d^+-axis is aligned with the positive-sequence stator voltage vector $\boldsymbol{V}_{sd+}^{+}$ in the SVO, which means $\boldsymbol{V}_{sq+}^{+}=\boldsymbol{0}$, thus with maintaining the constant electromagnetic torque selected as the control aim for rotor-side converter, the rotor current references can be obtained as

$$\boldsymbol{I}_{rd+}^{+*}=L_s\boldsymbol{V}_{sd+}^{+}P_{s0}/(L_m D_1), \tag{8a}$$

$$\boldsymbol{I}_{rq+}^{+*}=-L_s\boldsymbol{V}_{sd+}^{+}(Q_{s0}+D_2L_s^{-1})/(L_m D_2), \tag{8b}$$

$$\boldsymbol{I}_{rd-}^{-*}=k_{dd}\boldsymbol{I}_{rd+}^{+*}+k_{qd}\boldsymbol{I}_{rq+}^{+*}, \tag{8c}$$

$$\boldsymbol{I}_{rq-}^{-*}=k_{qd}\boldsymbol{I}_{rd+}^{+*}-k_{dd}\boldsymbol{I}_{rq+}^{+*}, \tag{8d}$$

where

$$D_1=(\boldsymbol{V}_{sd+}^{+})^2+(\boldsymbol{V}_{sd-}^{-})^2+(\boldsymbol{V}_{sq-}^{-})^2,$$

$$D_2=(\boldsymbol{V}_{sd+}^{+})^2-[(\boldsymbol{V}_{sd-}^{-})^2+(\boldsymbol{V}_{sq-}^{-})^2],$$

$$k_{dd}=\boldsymbol{V}_{sd-}^{-}/\boldsymbol{V}_{sd+}^{+},\quad k_{qd}=\boldsymbol{V}_{sq-}^{-}/\boldsymbol{V}_{sd+}^{+}.$$

Once the rotor current references are obtained for the selected control target, $\boldsymbol{I}_{rd+}^{+}$, $\boldsymbol{I}_{rq+}^{+}$, $\boldsymbol{I}_{rd-}^{-}$ and $\boldsymbol{I}_{rq-}^{-}$ are required to follow them precisely. Good control performance depends on the accurate decoupling of the *d*-*q* components and the removal of the impact from the network voltage disturbances. The typical control design at the grid voltage unbalance conditions employs two current controllers implemented in the positive and negative synchronous reference frames, respectively (Chomat *et al*., 2002; Jang *et al*., 2006; Hu *et al*., 2007; Wang and Xu, 2007; Xu and Wang, 2007). However, the positive- and

negative-sequence components of the rotor currents have to be decomposed from the measured originals. Since the decomposing process involves considerable time delay and leads to some errors in amplitude and phase, the systems cannot be fully decoupled during the transient conditions. As a result, the system performance and the system stability are all degraded. Furthermore, even when the network is perfectly balanced, the control system still has to perform the decomposition of the current and voltage, and then execute positive and negative sequence currents control. This unnecessarily deteriorates the dynamic performance of the overall system.

In order to overcome the aforementioned problems, a new control design is developed. The proposed control system consists of a proportional (P) controller and two harmonic resonant (R) controllers tuned in the frequencies of $\omega_{\text{slip+}}$ and $\omega_{\text{slip–}}$, respectively, which is implemented in the rotor rotating $\alpha_\text{r}\beta_\text{r}$ reference frame without a band-trap filter for rotor current decomposition. Hence, the proposed current controller can directly regulate the negative-sequence components as precisely and quickly as the positive-sequence without sacrificing the current regulator bandwidth caused by band-trap filters.

As shown in Eq.(7), it is obvious that under unbalanced grid voltage conditions, the voltage, current and flux in the $\alpha_\text{r}\beta_\text{r}$ reference frame all contain the AC quantities of both positive- and negative-sequence components with the frequencies of $\omega_{\text{slip+}}$ and $\omega_{\text{slip–}}$, respectively. Hence two resonant controllers tuned in the frequencies of $\omega_{\text{slip+}}$ and $\omega_{\text{slip–}}$, respectively, are needed to provide capability of operating with both the positive- and negative-sequence rotor currents $\boldsymbol{I}^{+}_{\text{r}dq+}\text{e}^{\text{j}\omega_{\text{slip+}}t}$ and $\boldsymbol{I}^{-}_{\text{r}dq-}\text{e}^{\text{j}\omega_{\text{slip–}}t}$, and to provide zero steady-state error for them. A PR rotor current controller in the $\alpha_\text{r}\beta_\text{r}$ reference frame, suitable for directly regulating the positive- and negative-sequence rotor current components, is shown in Fig.3.

Based on Eq.(5), the DFIG system during network voltage unbalance can be represented in the $\alpha_\text{r}\beta_\text{r}$ reference frame as

$$\frac{\text{d}}{\text{d}t}\boldsymbol{I}^{\text{r}}_{\text{r}\alpha\beta}=\frac{1}{\sigma L_\text{r}}\boldsymbol{V}^{\text{r}}_{\text{r}\alpha\beta}-\frac{1}{\sigma L_\text{r}}R_\text{r}\boldsymbol{I}^{\text{r}}_{\text{r}\alpha\beta}-\frac{L_\text{m}}{\sigma L_\text{r}L_\text{s}}\left(\boldsymbol{V}^{\text{r}}_{\text{s}\alpha\beta}-R_\text{s}\boldsymbol{I}^{\text{r}}_{\text{s}\alpha\beta}-\text{j}\omega_\text{r}\boldsymbol{\psi}^{\text{r}}_{\text{s}\alpha\beta}\right),\tag{9}$$

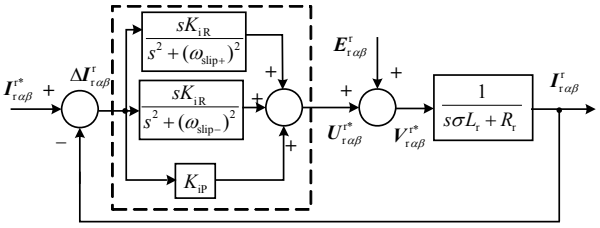

Fig.3 Current control diagram based on the Proportional plus Resonant (PR) controller

where $\boldsymbol{V}^{\text{r}}_{\text{r}\alpha\beta}$ is referred to as the rotor control voltage, produced by the PR controller, and designed as

$$\boldsymbol{V}^{\text{r}}_{\text{r}\alpha\beta}=\sigma L_\text{r}\boldsymbol{U}^{\text{r}}_{\text{r}\alpha\beta}+\boldsymbol{E}^{\text{r}}_{\text{r}\alpha\beta},\tag{10}$$

where

$$\boldsymbol{U}^{\text{r}}_{\text{r}\alpha\beta}=\frac{\text{d}}{\text{d}t}\boldsymbol{I}^{\text{r}}_{\text{r}\alpha\beta}=C_\text{PR}(s)(\boldsymbol{I}^{\text{r}*}_{\text{r}\alpha\beta}-\boldsymbol{I}^{\text{r}}_{\text{r}\alpha\beta}),$$

$$C_\text{PR}(s)=K_\text{iP}+\frac{sK_\text{iR}}{s^2+2\omega_\text{c}s+(\omega_{\text{slip+}})^2}+\frac{sK_\text{iR}}{s^2+2\omega_\text{c}s+(\omega_{\text{slip–}})^2},\tag{11}$$

and

$$\boldsymbol{E}^{\text{r}}_{\text{r}\alpha\beta}=(\boldsymbol{V}^{\text{r}}_{\text{s}\alpha\beta}-R_\text{s}\boldsymbol{I}^{\text{r}}_{\text{s}\alpha\beta}-\text{j}\omega_\text{r}\boldsymbol{\psi}^{\text{r}}_{\text{s}\alpha\beta})L_\text{m}/L_\text{s}$$

is defined as the equivalent rotor back electromagnetic force acting as a disturbance to the PR controller. K_iP and K_iR are the proportional and resonant parameters, respectively. K_iP plays the same role as for a PI regulator, which basically determines the system dynamics in terms of bandwidth, phase and gain margin. While the resonant controller with K_iR provides adequate gain for the components with the AC frequencies of $\omega_{\text{slip+}}$ and $\omega_{\text{slip–}}$, respectively, as shown in Fig.4, in which $\omega_{\text{slip+}}=20\pi$ and $\omega_{\text{slip–}}=220\pi$ for the simulated DFIG system due to ω_r=1.2 p.u. in this work. As a result, the PR controller is only relatively sensitive to the change of $\omega_{\text{slip+}}$ and $\omega_{\text{slip–}}$, which can be precisely gained via Phase-Lock Loop (PLL) and DFIG speed encoder. Besides, in order to reduce the sensitivity towards slight frequency variations in a typical wind-farm connected grid, a component with cutoff frequency of ω_c can be inserted into the resonant part to widen its frequency bandwidth (Teodorescu *et al*., 2006), as shown in Fig.4.

Based on the control strategy presented above, an unbalanced control scheme for the wind-turbine driven DFIG system under unbalanced grid voltage

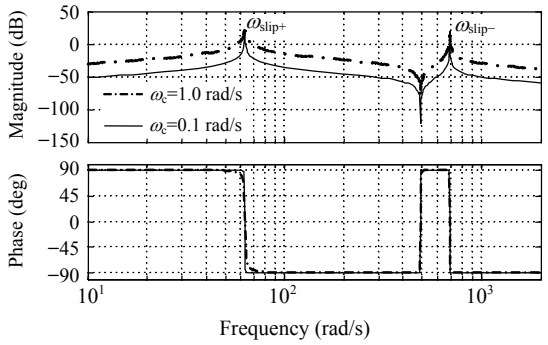

Fig.4 Bode plots of resonant controllers for regulating harmonics at the frequencies of $\omega_{slip+}=20\pi$ and $\omega_{slip-}=220\pi$, with $K_{iR}=1$, $\omega_c=0.1$ rad/s and 1.0 rad/s

conditions was constructed, as shown in Fig.5. As can be seen from the figure, a PLL circuit is used to detect the grid voltage frequency and to follow its phase, which provides dependency for implementing the positive and negative synchronous transformation of the stator and rotor voltages and currents.

The measured three-phase rotor currents are directly transformed into the $\alpha_r\beta_r$ reference frame. The obtained AC signals are composed of the positive- and negative-sequence components $\boldsymbol{I}^{+}_{rdq+}e^{j\omega_{slip+}t}$ and $\boldsymbol{I}^{-}_{rdq-}e^{j\omega_{slip-}t}$, without being decomposed separately into the positive- and negative-sequence ones. However, the four current references $\boldsymbol{I}^{+*}_{rd+}$, $\boldsymbol{I}^{+*}_{rq+}$, $\boldsymbol{I}^{-*}_{rd-}$, $\boldsymbol{I}^{-*}_{rq-}$, calculated corresponding to the selected control target, are all DC signals separated in the positive and negative synchronous frames. Therefore, in order to make the calculated current references match with the measured ones in the same reference frame, the reference currents should be transformed in the same manner as the measured ones. The associated transformation was marked as "Reference frame transformation" block in Fig.5.

SIMULATION INVESTIGATION

Simulations of the proposed control strategies for a DFIG-based wind power generation system were conducted by using Matlab/Simulink. The DFIG is rated at 1.5 MW and its parameters are listed in Table 1. Fig.6 shows the schematic diagram of the tested system. A single-phase load at the primary side of the coupling transformer is used to generate the voltage unbalance. The nominal DC-link voltage was 1200 V and the switching frequencies for both converters were 3 kHz. Since the large inertia of wind turbines results in a pretty slow change in rotor rotation, the DFIG speed was assumed to be fixed at 1.2 p.u. during simulations.

Tests on the system control and operation during relatively large transient network unbalance were carried out to demonstrate the validity of the proposed rotor current PR controller. The results are shown in Fig.7 for the transient stator voltage unbalance of

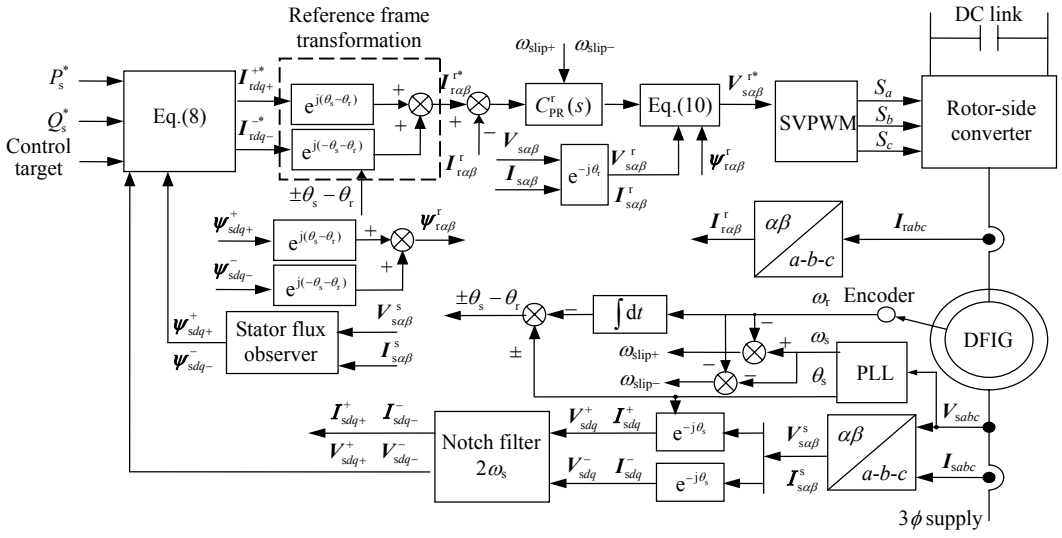

Fig.5 The diagram of the proposed unbalanced control strategy for DFIG under generalized unbalanced grid voltage conditions

Table 1 Parameters of the simulated DFIG

Parameter	Value
Rated power	1.5 MW
Stator voltage	575 V
Stator/rotor turns ratio	0.38
Stator resistance R_s	0.00706 p.u.
Rotor resistance R_r	0.005 p.u.
Stator leakage inductance $L_{\sigma s}$	0.171 p.u.
Rotor leakage inductance $L_{\sigma r}$	0.156 p.u.
Mutual inductance L_m	2.9 p.u.
Lumped inertia const.	5.04 s

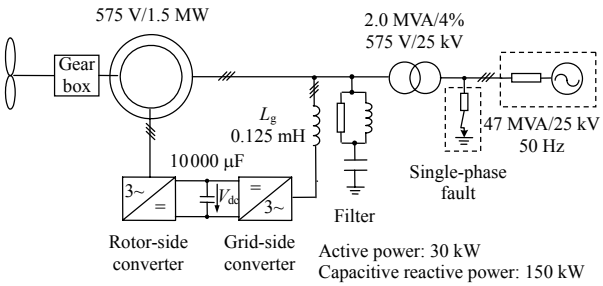

Fig.6 Schematic diagram of the tested system

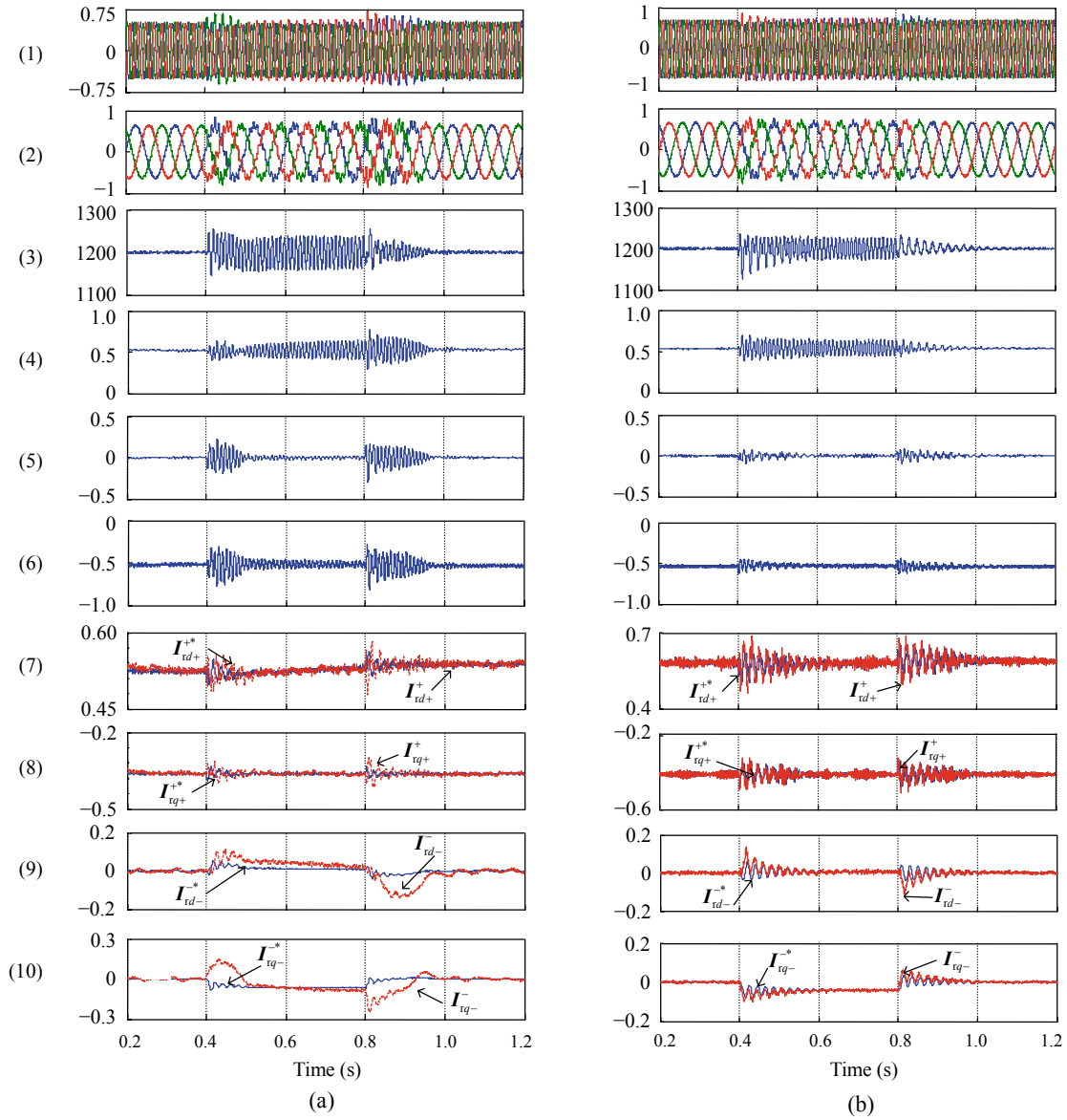

Fig.7 Simulated results under transient 10% unbalance stator voltage during 0.4~0.8 s. (a) With dual-PI rotor current controller; (b) With PR rotor current controller

(1) Three-phase stator currents (p.u.); (2) Three-phase rotor currents (p.u.); (3) Converter DC-link voltage (V); (4) Stator output active power (p.u.); (5) Stator output reactive power (p.u.); (6) DFIG electromagnetic torque (p.u.); (7) Rotor positive-sequence *d*-axis current (p.u.); (8) Rotor positive-sequence *q*-axis current (p.u.); (9) Rotor negative-sequence *d*-axis current (p.u.); (10) Rotor negative-sequence *q*-axis current (p.u.)

10% appearing at the instant of 0.4 s and removed at 0.8 s. For this case, the grid-side converter was controlled to maintain DC-link voltage flat (Hu and He, 2007) and, the rotor-side converter was designed to flatten electromagnetic torque so as to reduce the mechanical press on the wind turbines. The stator active and reactive power references were kept 0.55 p.u. and 0 p.u., respectively. Fig.7a shows the simulated results using the dual-PI rotor current controllers based on the decomposition of the positive- and negative-sequence rotor currents (Hu *et al*., 2007). Since the decomposing process, which is absolutely necessary for the dual PI regulator, involves considerable time delay and leads to some errors in the amplitude and phase with respect to the composed signals, the rotor current could not be regulated fleetly and precisely during transients, especially for the negative-sequence components, as shown in Fig.7a (9)(10). As a result, the whole control performance was deteriorated during transient conditions, as shown in Fig.7a (1)~(6).

For comparison, using the proposed PR rotor current controller, Fig.7b shows the simulated results with the same operation condition as in Fig.7a. From the results it can be clearly seen that the negative-sequence rotor currents are immediately regulated precisely in case of the voltage unbalance occurring, as shown in Fig.7a (9)(10). When the unbalance was cleared at 0.8 s, the proposed PR design also provided pretty good current regulating and the system went back to the normal operation mode smoothly, as shown in Fig.7b (1)~(6).

CONCLUSION

An adaptive rotor current controller for wind-turbine driven DFIG was proposed. The controller consists of a proportional regulator and two harmonic resonant controllers implemented in the rotor rotating reference frame. The two resonant controllers were tuned at slip frequencies ω_{slip+} and ω_{slip-}, respectively. As a result, the positive- and negative-sequence components of the rotor current are fully regulated by the proposed PR controller without involving the positive- and negative-sequence decomposition, which in effect improves the fault ride-through capability of the DFIG-based wind power generation system during the period of relatively large transient grid voltage unbalance.

References

Brekken, T., Mohan, N., 2003. A Novel Doubly-Fed Induction Wind Generator Control Scheme for Reactive Power Control and Torque Pulsation Compensation Under Unbalanced Grid Voltage Conditions. IEEE 34th Annual Power Electronics Specialist Conf., p.760-764.

Brekken, T., Mohan, N., Undeland, T., 2005. Control of a Doubly-Fed Induction Wind Generator Under Unbalanced Grid Voltage Conditions. Proc. European Conf. on Power Electronics and Applications.

Chomat, M., Bendl, J., Schreier, L., 2002. Extended Vector Control of Doubly Fed Machine Under Unbalanced Power Network Conditions. Proc. IEEE Int. Conf. on Power Electronics, Machines and Drives, p.329-334. [doi:10.1049/cp:20020138]

Hu, J.B., He, Y.K., 2007. Multi-frequency proportional-resonant (MFPR) current controller for PWM VSC under unbalanced supply conditions. *J. Zhejiang Univ. Sci. A*, **8**(10):1527-1531. [doi:10.1631/jzus.2007.A1527]

Hu, J.B., He, Y.K., Nian, H., 2007. Enhanced control of DFIG-used back-to-back PWM VSC under unbalanced grid voltage conditions. *J. Zhejiang Univ. Sci. A*, **8**(8):1330-1339. [doi:10.1631/jzus.2007.A1330]

Jang, J., Kim, Y., Lee, D., 2006. Active and Reactive Power Control of DFIG for Wind Energy Conversion Under Unbalanced Grid Voltage. Power Electronics and Motion Control Conf., CES/IEEE 5th Int. (IPEMC'06), p.1-5. [doi:10.1109/IPEMC.2006.297323]

Teodorescu, R., Blaabjerg, F., Liserre, M., Loh, P.C., 2006. Proportional-resonant controllers and filters for grid-connected voltage-source converters. *IEE Proc. Electric Power Appl.*, **153**(5):750-762. [doi:10.1049/ip-epa:20060008]

Wang, Y., Xu, L., 2007. Control of DFIG-based Wind Generation Systems Under Unbalanced Network Supply. IEEE Int. Electric Machines & Drives Conf., p.430-435. [doi:10.1109/IEMDC.2007.382706]

Xu, L., Wang, Y., 2007. Dynamic modeling and control of DFIG based wind turbines under unbalanced network conditions. *IEEE Trans. on Power Syst.*, **22**(1):314-323. [doi:10.1109/TPWRS.2006.889113]